Forecasting Repair and Maintenance Services of Medical Devices Using Support Vector Machine

Hao-yu Liao
Department of Environmental Engineering Sciences,
University of Florida,
Gainesville, FL 32611
e-mail: haoyuliao@ufl.edu

Willie Cade
ICR Management,
Chicago, IL 60618
e-mail: williecade@gmail.com

Sara Behdad[1]
Department of Environmental Engineering Sciences,
University of Florida,
Gainesville, FL 32611
e-mail: sarabehdad@ufl.edu

Accurate prediction of product failures and the need for repair services become critical for various reasons, including understanding the warranty performance of manufacturers, defining cost-efficient repair strategies, and compliance with safety standards. The purpose of this study is to use machine learning tools to analyze several parameters crucial for achieving a robust repair service system, including the number of repairs, the time of the next repair ticket or product failure, and the time to repair. A large data set of over 530,000 repairs and maintenance of medical devices has been investigated by employing the Support Vector Machine (SVM) tool. SVM with four kernel functions is used to forecast the timing of the next failure or repair request in the system for two different products and two different failure types, namely, random failure and physical damage. Frequency analysis is also conducted to explore the product quality level based on product failure and the time to repair it. Besides, the best probability distributions are fitted for the failure count, the time between failures, and the time to repair. The results reveal the value of data analytics and machine learning tools in analyzing post-market product performance and the cost of repair and maintenance operations. [DOI: 10.1115/1.4051886]

Keywords: machine learning, support vector machine, repair, maintenance, forecasting, medical devices, process planning, sustainable manufacturing

1 Introduction

Most products experience some sort of failure during their lifespan. Several reasons for product failures include insufficient reliability, poor quality, wrong design, uncertain usage, and production conditions [1]. Product failure can cause adverse effects such as financial cost, consumer dissatisfaction, and ruining manufacturers' market image [2]. Product repair is often part of the product lifecycle events. For example, once the product reaches the end-of-use or the end-of-life, customers may decide to upgrade their product due to technological advances or repair, refurbish, or remanufacturer to extend the product lifespan [3].

The concept of end-of-use product recovery and extending the product lifecycle is nothing new in the literature. Previous studies have already discussed product recovery challenges that are facing different industries, such as building material stocks [4], automobiles [5], and household electric and electronic equipment [6]. Mathematical models have been developed to overcome some of those challenges (e.g., uncertain quality and quantity of waste stream) and help remanufacturers decide what to do with used devices [7,8].

Among the six common recovery strategies (e.g., reuse, repair, recondition/refurbishment, remanufacturing, cannibalization, and material recovery), repair has received less attention in the literature. However, predicting product failure has always been of interest to both academia and industry. Several studies have discussed the forecasting of product failure. To name a few, Yoon and Sohn built several random-effects regression models to forecast the mean time between failure (MTBF) [9]. Al-Garni et al. used the Weibull family to build a relationship with aircraft air-conditioning failure [10]. Wang and Yuan completed the failure rate prediction based on the AR model [11]. Wang and Yin adopted Weibull distribution to failure rate prediction [12]. Sexton et al. used different rules such as single-tag and rules-based to extract keywords to estimate median time to failure [13]. Brundage et al. also studied technical language processing by considering human-in-the-loop, natural language processing tools, and text analysis to analyze documents that contain the equipment maintenance data [14]. While the previous studies have discussed product failure and maintenance, the number of studies that have worked with real industry data sets is very limited. The practical insights derived from analyzing big industry data sets help us define proper repair and maintenance strategies for corporations toward cost reduction and sustainability goals.

This study aims to show how machine learning tools can help businesses analyze the overwhelming data set of product post-market performance and identify the depth and significance of the demand for repair and maintenance services. The Support Vector Machine (SVM) regression model simulates the product failure scenario and predicts the timing of the next repair service. The forecasting accuracy of SVM in regression is already confirmed by several studies [15–17]. In this study, the data set is collected from 2004 to 2018 under different management policies. Although some bias and data set noise influence the decision to repair, the SVM model can still forecast failure time.

Besides, this study runs a frequency analysis to analyze the product quality based on the probability distributions of failure count, TBF, and time to repair (TTR). The frequency analysis provides information about each product maintenance condition.

This study provides an overview of products maintenance conditions by frequency analysis and offers a way to forecast product failure and the timing of the subsequent repair service request. Figure 1 shows the overall structure of this study.

2 Overview of Data Set

2.1 Elements of the Data Set. In the current study, we investigate 536,597 records of repair and maintenance of medical devices, 90,278 individual products, and 9,351 product types from 2004 to 2018. The management policies may affect the collection and documentation of the repair data set and might have

[1]Corresponding author.

Manuscript received July 5, 2021; final manuscript received July 19, 2021; published online August 16, 2021. Tech. Editor: Y. Lawrence Yao.

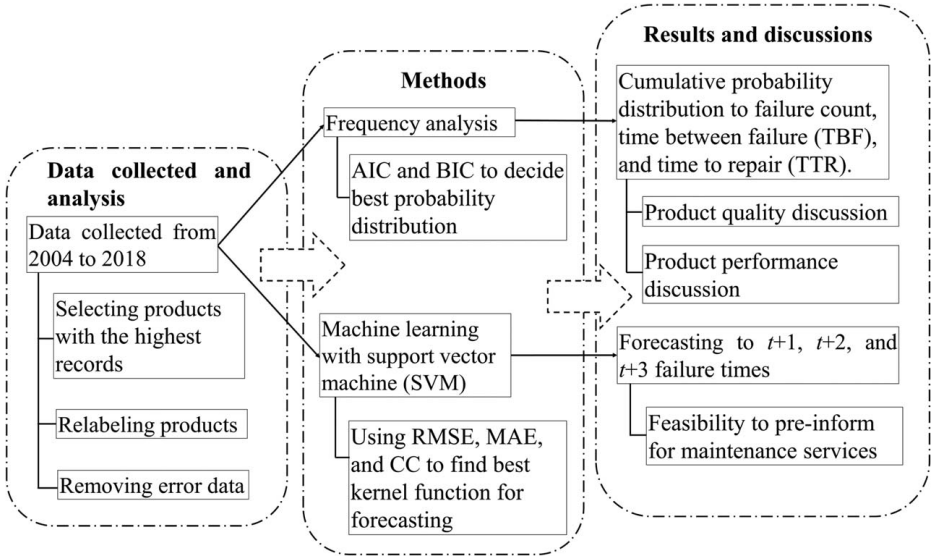

Fig. 1 The general data collection and analysis procedure of this study

imposed some biases in how the data are reported. The data come from one of the largest health care providers in the United States. The data set includes 9351 different products with different functions and purposes, such as infusion pumps, pulse detection, and oximeters. The average number of repair orders is 35,773 per year or 98 repair orders per day. Therefore, the need for a maintenance plan is significant for the health care provider.

Table 1 shows an overview of the available fields of data for each repair and maintenance record. First Asset Number is the unique code to identify an individual product. First Asset Description is the information of product function, and First Asset Model Number is the name of each type of product. Date Created and Completed Date fields are the start time and the completion time on the repair. Based on the Date Created and Completed Date, we can identify TBF and TTR. The TBF is the time between an individual product's failures, and the TTR is the repair start time to repair completion time. TBF and TTR are good indicators of product reliability and cost of repair. The long TBF and short TTR mean that a product has high reliability and may be easier to be maintained.

Figure 2 shows the distribution of 35 repair reasons among the top 10 product categories. We have only relabeled the equipment names, including CA type 1, CA type 2, M8 type 1, PA type 1, PC type 1, MF type 1, CSE type 1, VE type 1, R type 1, and M8 type 2. We have not relabeled the repair codes, such as failure reasons and product type, to train the models. As shown in Fig. 2, 35 repair reasons are listed for the relabeled products. The repair attributes field in the data set provides specific details on why an individual product needs repair. For example, random failure (RF) is a physical failure with excessive stress of the device and can happen at any time [18,19].

Figures 3 and 4 show the number of RF and physical damage (PD) for the top 10 categories of products, respectively. The top 10 categories of products have the highest records of data among all 9351 product types. Among the top 10 categories, the CA type 1 and CA type 2 are selected for the forecasting part of the study due to enough sample size. The number of RF and PD is the highest among other failure reasons.

According to Table 2, some product categories serve the same functions. For example, there are many products with infusion pumps and multitherapy functions. Four product categories, including CA type 1, M8 type 1, PA type 1, and M8 type 2, have the same function.

Table 1 The description of data set fields

Data attribute	Description
1. Work order number	The work order of repair
2. Type code	Product type
3. First asset number	Property unique number
4. First asset description	Function of product
5. First asset manufacturer name	Manufacturer
6. First asset model number	Product name
7. First asset serial number	Unique serial number
8. Date created	Repair start time
9. Completed date	Repair completion time
10. Repair attribute	The reason for repair

2.2 Data Frequency Analysis. This section describes the frequency analysis of the failure count, TBF, and TTR. To analyze the reliability based on the above indices, we need to fit the best probability distribution for each product type. In the previous studies, Patil applied Normal, Lognormal, and Weibull distributions to reliability and maintainability analysis on hardware and software failures [20]. Lampreia et al. used the Weibull probability density function to analyze MTBF on the reliability analysis [21]. Sukhwani et al. applied Gamma distribution to analyze the reliability of NASA space flight software [22]. Tronskar et al. analyzed corrosion damage for pipelines and pressure vessels by using Gumbel distribution [23]. Four probability distributions, including Gumbel, Gamma, Normal, and Weibull distributions, have been applied to this study. The frequency analysis is also conducted for five categories of products: CA type 1, CA type 2, M8 type 1, PA type 1, and M8 type 2.

The best-fitted probability distributions for the failure count, TBF, and TTR are determined by the Akaike information criterion (AIC) and Bayesian information criterion (BIC). The AIC test that measures the discrepancy between the true model and simulated model is proposed by Akaike (1973) [24], and the BIC test is based on the Bayesian framework [25]. Several studies had applied the AIC or BIC to compute the best-fitted probability distributions and showed the AIC and BIC are good indices for this purpose [26–29]. The probability distribution with the minimum AIC and BIC, among other distributions, is the best-fitted distribution. The AIC is constituted by the principle of maximum

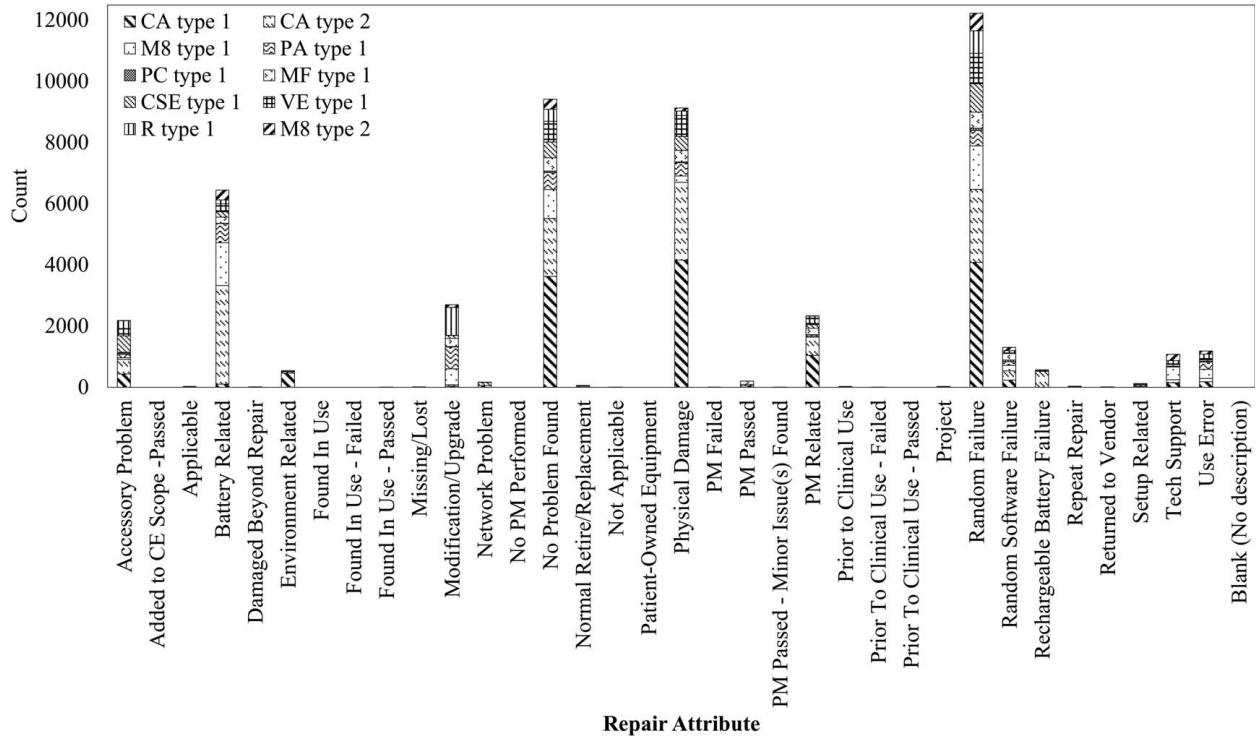

Fig. 2 Summary of all repair types for all products and showing the count of top 10 products (among the repair reasons, most repair records are the RF)

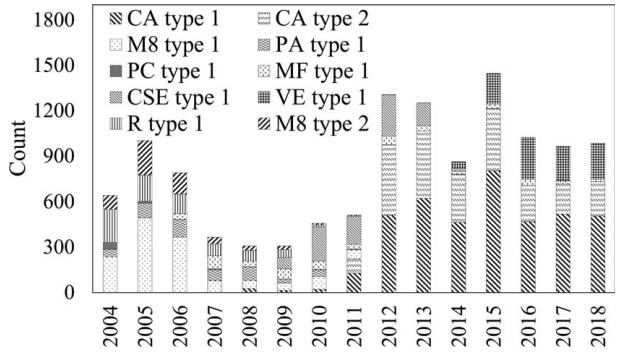

Fig. 3 The number of RF for the top 10 product types over time

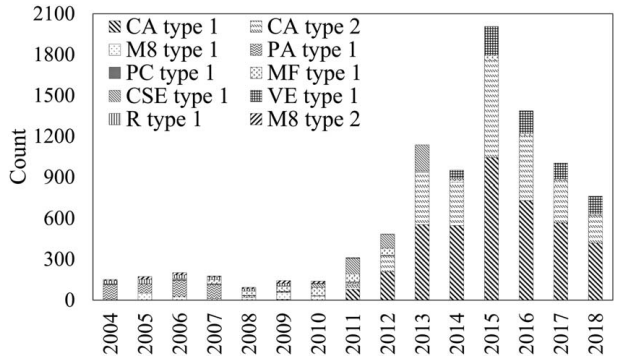

Fig. 4 The number of PD for the top 10 product types over time

entropy and is expressed as

$$AIC = 2n - 2\ln(\hat{h}) \tag{1}$$

where $\hat{h}$ indicates the maximum value of the likelihood function, and n is the number of probability distribution parameters. The BIC is constructed by the Bayesian framework and is given as

$$BIC = \ln(s)n - 2\ln(\hat{h}) \tag{2}$$

where s expresses the number of samples.

Table 3 shows the best-fitted probability distributions of RF and PD. As seen, the best-fitted probability distributions are either Weibull or Gamma. It is reasonable as the histograms of failure count, TBF, and TTR are similar to exponential shape. The example shown in Figs. 5 and 6 illustrates the probability density function (PDF) and the cumulative distribution function (CDF) of failure count for RF in CA type 2.

Table 4 represents the frequency analysis results for RF and PD with the best-fitted PDF. The $P(X \geq 1)$ for failure count means the probability that at least one failure happens. For TBF, it means the probability that an individual product has a normal operation of at least one year before it is broken. For TTR, it means the probability that an individual product needs at least ten days to be repaired.

Table 2 The summary of function for the top 10 product categories

Product	First asset description
CA type 1	Infusion Pumps, Multitherapy
CA type 2	Controllers, Infusion Pump Systems, Programmable
M8 type 1	Infusion Pumps, Multitherapy
PA type 1	Infusion Pumps, Multitherapy
PC type 1	Hospital Communication Systems, Nurse Call
MF type 1	Infusion Pumps, Multitherapy, Syringe
CSE type 1	Circulatory Assist Units, Peripheral Compression, Sequential
VE type 1	Circulatory Assist Units, Peripheral Compression, Sequential
R type 1	Oximeters, Pulse
M8 type 2	Infusion Pumps, Multitherapy

Table 3 The best-fitted probability distribution of RF and PD

Product	Failure count	TBF (year)	TTR (10 days)
CA type 1	Wei, Wei AIC: 4922, 737 BIC: 2947, 763	Gam, Gam AIC: 926, 585 BIC: 944, 604	Wei, Wei AIC: 3653, 5411 BIC: 3679, 5437
CA type 2	Wei, Wei AIC: 1819, 583 BIC: 1842, 907	Wei, Gam AIC: 604, 606 BIC: 627, 622	Wei, Wei AIC: 6981, 4670 BIC: 7005, 4688
M8 type 1	Wei, Wei AIC: 2109, 373 BIC: 2130, 387	Wei, Gam AIC: 570, 342 BIC: 595, 346	Wei, Wei AIC: 36948, 485 BIC: 36975, 465
PA type 1	Wei, Wei AIC: 398, 410 BIC: 415, 427	Gam, Gam AIC: 542, 461 BIC: 553, 471	Wei, Wei AIC: 664, 999 BIC: 681, 1015
M8 type 2	Wei, Wei AIC: 1388, 530 BIC: 1401, 540	Gam, Gam AIC: 491, 445 BIC: 508, 446	Wei, Wei AIC: 5208, 13214 BIC: 5225, 1325

Note: wei, weibull; gam, gamma.

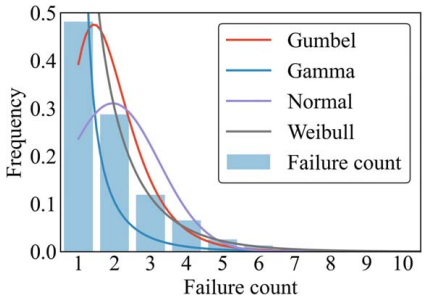

Fig. 5 Four fitted PDF of failure count for RF of CA type 2

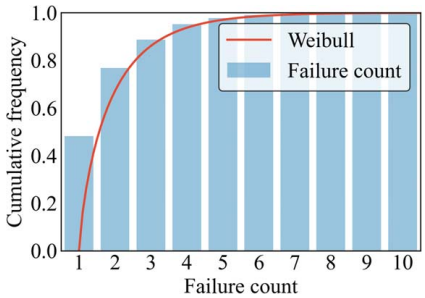

Fig. 6 Best-fitted CDF of failure count for RF of CA type 2

Comparing the failure count of RF and PD, the overall probability of RF is larger than PD. For example, the $P(X \geq 1)$ to $P(X \geq 5)$ of CA type 1 is from 100% to 25% on RF but is from 100% to 2% on PD. It reveals that random failure is the most repair reason for these products. The $P(X \geq 1)$ and $P(X \geq 2)$ of CA type 1 to CA type 2 on RF are almost similar, but the $P(X \geq 3)$ to $P(X \geq 5)$ of CA type 2 is smaller than that of CA type 1. It means that CA type 2 is more stable than CA type 1. Also, comparing CA type 1, M8 type 1, PA type 1, and M8 type 2 under the same functional purposes (Infusion Pumps, Multitherapy) on RF, the PA type 1 is more reliable among these products. Although $P(X \geq 4)$ and $P(X \geq 5)$ of PA type 1 are slightly higher than those of M8 type 1, the overall $P(X \geq 2)$ to $P(X \geq 3)$ are smaller among the same functional products. M8 type 2 is not reliable among products with the same function since it has a high-value $P(X \geq 2)$. Almost 77% of M8 type 2 products fail at least twice.

The overall $P(X \geq 1)$ to $P(X \geq 5)$ for TBF among RF and PD are very similar. The TBF reveals that products can normally operate at least 1 year to 3 years before they fail. CA type 1 and PA type 1 have higher $P(X \geq 1)$ on RF among all products. It means that CA type 1 and PA type 1 have higher probabilities of operating for more than 1 year, among others. M8 type 2 can endure more PD because it has a higher probability of $P(X \geq 1)$ to $P(X \geq 3)$ than others with the same functional purpose.

Table 4 The probability (0 ~ 100%) of RF and PD considering the best-fitted pdf: $P(X \geq 1)$ to $P(X \geq 5)$

	Random failure, physical damage				
Product	$P(X \geq 1)$	$P(X \geq 2)$	$P(X \geq 3)$	$P(X \geq 4)$	$P(X \geq 5)$
Failure count					
CA type 1	100, 100	40, 32	32, 13	28, 5	25, 2
CA type 2	100, 100	33, 30	14, 12	6, 5	3, 2
M8 type 1	100, 100	43, 14	26, 9	17, 6	12, 5
PA type 1	99, 100	29, 22	26, 7	24, 2	23, 1
M8 type 2	94, 100	77, 07	55, 2	37, 0	24, 0
TBF (year)					
CA type 1	51, 53	29, 27	16, 13	9, 6	5, 3
CA type 2	44, 55	23, 27	12, 13	7, 6	4, 3
M8 type 1	39, 58	19, 36	10, 22	5, 14	3, 9
PA type 1	50, 45	28, 24	16, 13	9, 7	6, 4
M8 type 2	38, 68	17, 42	8, 23	3, 12	2, 6
TTR (10 days)					
CA type 1	40, 31	33, 22	29, 17	26, 14	24, 12
CA type 2	25, 22	19, 15	15, 11	12, 09	11, 7
M8 type 1	31, 46	19, 27	13, 17	9, 11	7, 7
PA type 1	20, 2	10, 0.3	6, 0	4, 0	3, 0
M8 type 2	39, 66	30, 50	26, 39	23, 31	21, 26

The TTR results reveal that CA type 1 and M8 type 2 are not easy to repair among all products. These two products have higher $P(X \geq 1)$ to $P(X \geq 5)$ than others, especially in $P(X \geq 5)$. Once a random failure occurs, it takes up to 50 days to repair the device. Also, CA type 1, M8 type 2, and M8 type 1 take a longer time to repair in the case of PD. Therefore, the cost of repair is likely higher for CA type 1 and M8 type 2. In contrast, PA type 1 is easier to be repaired among other products. Therefore, after analyzing Table 4, the PA type 1 category is more cost-effective for Infusion Pumps and Multitherapy functions.

3 Method: Support Vector Machine

Vapnik proposed support vector networks in 1995 to solve the classification problem and later developed it for regression analysis [30]. SVM has confirmed its forecasting accuracy through previous work [15–17]. It has been applied to different fields for various predictions, such as dewpoint temperature prediction [31], stock prediction [32], and flood forecasting [16,33]. Further details on SVM can be found in Ref. [34].

According to Ref. [16], it is given the training set of $[(x_1, y_1), (x_2, y_2), (x_3, y_3), \ldots, (x_n, y_n)]$ with the input vector x and the target data y. The regression function can be expressed as

$$\hat{y} = f(x) = \boldsymbol{w}^T \Phi(x) + b \tag{3}$$

where $\hat{y}$ is the output, $\boldsymbol{w}$ is the weight, $\Phi(x)$ is a nonlinear function, and b is the bias. According to the structural risk minimization (SRM) principle, the $\boldsymbol{w}$ and b can be derived by minimizing the structural risk function as follows

$$Min\ R(w, b, \xi, \xi^*) = \frac{1}{2}\|\boldsymbol{w}\|^2 + c^* \sum_{i=1}^{n} L_e(\xi + \xi^*) \tag{4}$$

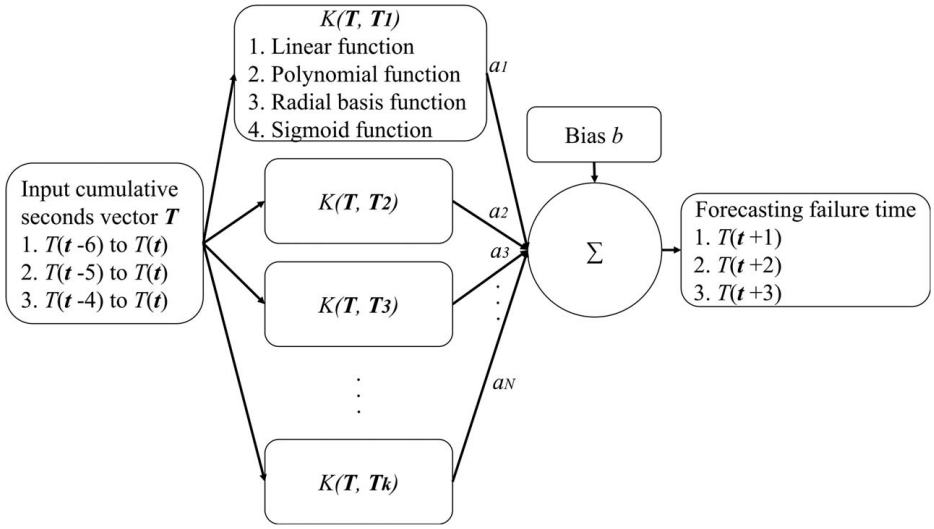

Fig. 7 The structure of the support vector machine

$$\text{Subject to } \begin{cases} y_i - \hat{y}_i = \hat{y}_i - (\boldsymbol{w}^T \Phi(x) + b) \le \varepsilon + \xi_i \\ y_i - \hat{y}_i = (\boldsymbol{w}^T \Phi(x) + b) - \hat{y}_i \le \varepsilon + \xi_i' \\ \xi_i \ge 0 \\ \xi_i' \ge 0 \\ i = 1,\ 2, \ldots,\ n \end{cases} \tag{5}$$

where c^* is a penalty parameter for making a tradeoff between model complexity, and ε is the error tolerance as a range between target data y and output data $\hat{y}$. ξ and ξ^* are slack variables. The Lagrange multipliers with a and a^* can be used to solve the above-mentioned optimization problem

$$f(x) = \sum_{i=1}^{v} (a_i - a_i^*) K(x_k, x) + b \tag{6}$$

where v is the number of support vector, x_k is the support vector, and $K(x_k, x)$ is a kernel function. SVM has four kernel functions as follows:

Linear function:

$$K(x_i, x_j) = x_i^T \cdot x_j \tag{7}$$

Polynomial function:

$$K(x_i, x_j) = (r \cdot x_i^T \cdot x_j + c)^d \tag{8}$$

Radial basis function:

$$K(x_i, x_j) = \exp(-r\|x_i - x_j\|^2) \tag{9}$$

Sigmoid function:

$$K(x_i, x_j) = \tanh(r \cdot x_i^T \cdot x_j + c) \tag{10}$$

where r is a scaling factor, c is the bias term, and d is the degree term. This study uses the grid search method [35] to find parameters (r, c^*, d, and ε). Figure 7 shows an overview of the SVM structure.

4 Forecasting the Time of Next Random Failure or Repair Service Ticket

4.1 The Input of Support Vector Machine. Four different kernel functions, including Linear (LN), Polynomial (PL), Radial basis (RBF), and Sigmoid (SIG) functions, are selected to see which one has better forecasting performance. The input variable to the SVM model is the cumulative seconds, as illustrated in Table 5. The definition of cumulative seconds is the difference between the current failure time and the subsequent failure time. We should note that the current and upcoming failures may not be for the same individual product. The output of SVM is the forecasted time of the next failure. When the failure time is $t+1$, $t+2$, or $t+3$, the SVM model will predict the next first, second, and third failure times in advance. The relationship of the failure time to the input factor is shown in Table 6. The $T(t)$, $T(t-1)$, and $T(t-2)$ denote current, previous, and the second-to-last product failure time as an input factor, respectively. This study selects $T(t-6)$, $T(t-5)$, $T(t-4)$, $T(t-3)$, $T(t-2)$, $T(t-1)$, $T(t)$ as input factors to forecast the time of the next failure since these input factors have a high correlation coefficient (CC) with output data. Also, when the time of failure increases, the number of input factors is reduced. The reason for reducing the input factor is to maintain the high correlation coefficient between input and output data.

We have selected two products, including CA type 1 and CA type 2, for prediction since these two products have enough sample sizes

Table 5 Example of calculating cumulative seconds (e.g., time of the first failure and the second failure)

Order	Failure time	Cumulative seconds
1	2008-07-23 11:00:00	0 s (Time 1–Time1)
2	2008-07-24 08:00:00	75600 s (Time 2–Time 1)
3	2008-07-28 09:00:00	424800 s (Time 3–Time 1)
4	2008-08-08 09:00:00	1375200 s (Time 4–Time 1)
5	2008-08-08 09:00:00	1375200 s (Time 5–Time 1)
6	2008-09-04 09:00:00	3708000 s (Time 6–Time 1)

Table 6 Basic information about CA type 1 and CA type 2

Information	CA type 1	CA type 2
Training RF data set	5141	3256
Testing RF data set	2203	1395
Data start time	2008-7-23 11:00:00	2011-6-25 14:00:00
Data end time	2018-12-31 8:14:23	2018-12-27 16:16:40
Data set length (years)	10.5	7.51
Failure time (order)	Input factor	
$t+1$	$T(t-6)$, $T(t-5)$, $T(t-4)$, $T(t-3,)$ $T(t-2)$, $T(t-1)$, $T(t)$	
$t+2$	$T(t-5)$, $T(t-4)$, $T(t-3,)$ $T(t-2)$, $T(t-1)$, $T(t)$	
$t+3$	$T(t-4)$, $T(t-3,)$ $T(t-2)$, $T(t-1)$, $T(t)$	

Table 7 The training and testing results for random failure in CA type 1

Failure time (order)	Train, test RMSE (s)	Train, test MAE (s)	Train, test CC
SVM-LN			
$t+1$	400871, 49757	116881, 40583	1.0, 1.0
$t+2$	518767, 61001	137235, 46601	1.0, 1.0
$t+3$	674727, 80082	156101, 55303	1.0, 1.0
SVM-PL			
$t+1$	316582, 41586	104599, 25892	1.0, 1.0
$t+2$	479382, 59246	126297, 43609	1.0, 1.0
$t+3$	587345, 72843	149849, 54131	1.0, 1.0
SVM-RBF			
$t+1$	657926, 180843	148978, 145477	1.0, 1.0
$t+2$	767078, 186720	166230, 153202	1.0, 1.0
$t+3$	869516, 210683	190072, 174058	1.0, 1.0
SVM-SIG			
$t+1$	561663, 68182	132766, 47432	1.0, 1.0
$t+2$	728044, 81871	160764, 57391	1.0, 1.0
$t+3$	820536, 89412	192585, 63175	1.0, 1.0

and are commonly used in medical applications. Table 6 shows the basic information for CA type 1 and CA type 2.

The proportion of training and test sample sizes is 7 and 3. The available data on the start time and the end time for CA type 1 and CA type 2 are from July 23, 2008, 11:00:00 to December 31, 2018, 8:14:23 and from June 25, 2011, 14:00:00 to December 27, 2018, 16:16:40, respectively. The length of the data set is at least 7.5 years for both products. The forecasting results will be discussed in Sec. 4.2.

4.2 The Forecasting Results for Random Failure. The training and testing results for SVM-LN, SVM-PL, SVM-RBF, and SVM-SIG are shown in Tables 7 and 8. According to the tables, the SVM-PL has better performance on training and testing, among other kernel functions. When the time is $t+1$, $t+2$, and $t+3$, both SVM-LN and SVM-PL can forecast the time of the next random failure for CA type 1 and CA type 2 shown in Figs. 8–11. The codes SVM-LN, SVM-PL, SVM-RBF, and SVM-SIG mean the kernel of SVM, including linear, polynomial,

Table 8 The training and testing results for random failure in CA type 2

Failure time (order)	Train, test RMSE (s)	Train, test MAE (s)	Train, test CC
SVM-LN			
$t+1$	107236, 98583	78451, 67329	1.0, 1.0
$t+2$	156948, 132817	126061, 105525	1.0, 1.0
$t+3$	181359, 162836	134489, 120174	1.0, 1.0
SVM-PL			
$t+1$	95388, 87427	71958, 56968	1.0, 1.0
$t+2$	133387, 124724	91799, 84560	1.0, 1.0
$t+3$	168557, 149977	132054, 119583	1.0, 1.0
SVM-RBF			
$t+1$	175961, 146894	118780, 113243	1.0, 1.0
$t+2$	201158, 167534	135506, 128570	1.0, 1.0
$t+3$	221640, 182546	150537, 143188	1.0, 1.0
SVM-SIG			
$t+1$	128303, 129916	88436, 88981	1.0, 1.0
$t+2$	171729, 146100	126134, 116760	1.0, 1.0
$t+3$	200389, 179164	142448, 132439	1.0, 1.0

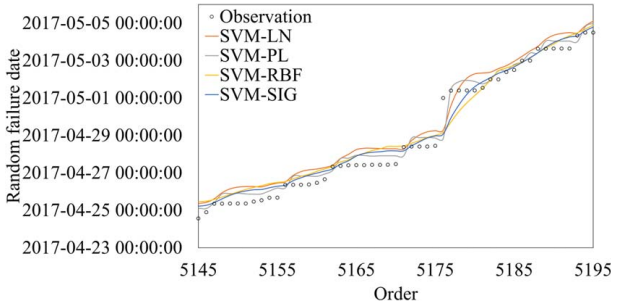

Fig. 8 Testing results of forecasting $t+1$ among all kernel functions for CA type 1

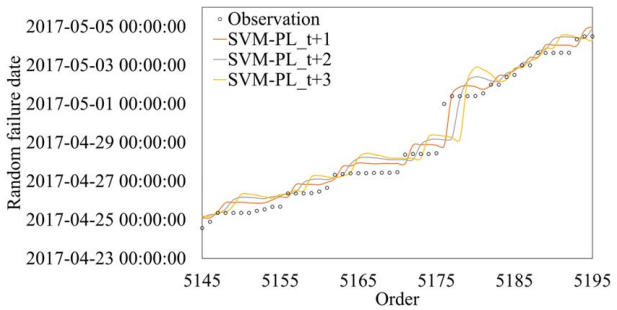

Fig. 9 Testing results of forecasting $t+1$ to $t+3$ with polynomial kernel function for CA type 1

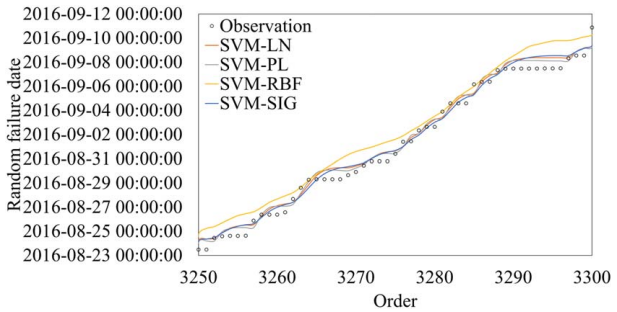

Fig. 10 Testing results of forecasting $t+1$ among all kernel functions for CA type 2

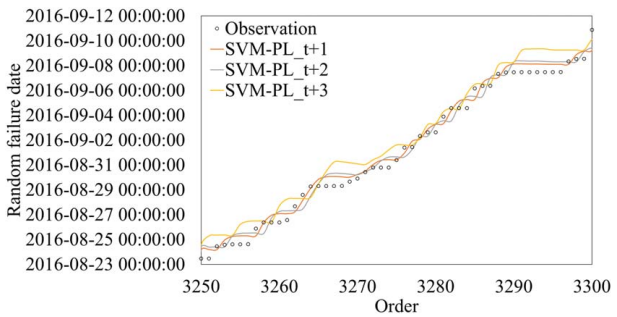

Fig. 11 Testing results of forecasting $t+1$ to $t+3$ with polynomial kernel function for CA type 2

radial basis, and sigmoid function, respectively. As time increases, it is obvious that the forecasting performance is decreased. Figures 9 and 11 provide specific details on the above-mentioned discussion. Based on Tables 7 and 8 and Figs. 8–11, the performance of SVM models with different kernel functions can forecast the next random failure without overfitting. For the indices such as root-mean-square-error (RMSE), mean absolute error (MAE), and

Table 9 The actual failure time and forecasting failure time with SVM-PL for orders 5184 to 5189 of CA type 1 and orders 3277 to 3283 of CA type 2

	Forecasting failure time		
Actual failure time	$t+1$	$t+2$	$t+3$
CA type 1			
2017-05-02 09:20:16	2017-05-02 11:29:20	2017-05-02 14:07:12	2017-05-02 06:36:32
2017-05-02 12:07:12	2017-05-02 19:00:00	2017-05-02 17:07:28	2017-05-02 20:07:44
2017-05-02 23:59:44	2017-05-02 22:45:04	2017-05-03 02:53:04	2017-05-02 21:14:56
2017-05-02 23:59:44	2017-05-03 09:38:24	2017-05-03 04:22:40	2017-05-03 05:08:00
2017-05-03 15:22:56	2017-05-03 10:00:48	2017-05-03 17:30:56	2017-05-03 09:15:28
2017-05-03 15:24:00	2017-05-04 01:01:36	2017-05-03 19:46:24	2017-05-03 20:53:36
CA type 2			
2016-09-01 10:28:00	2016-09-01 22:02:40	2016-09-01 06:14:08	2016-09-01 14:28:16
2016-09-02 08:08:16	2016-09-02 02:16:32	2016-09-02 06:30:08	2016-09-02 05:23:28
2016-09-02 15:09:52	2016-09-02 21:25:20	2016-09-02 08:03:44	2016-09-03 06:19:44
2016-09-02 15:10:40	2016-09-03 06:33:04	2016-09-03 06:19:44	2016-09-03 08:06:24
2016-09-03 21:29:52	2016-09-03 08:06:24	2016-09-03 13:40:32	2016-09-04 07:02:24
2016-09-04 13:56:16	2016-09-04 09:29:20	2016-09-03 13:27:12	2016-09-04 13:29:52
2016-09-04 14:02:24	2016-09-05 03:31:28	2016-09-04 19:30:40	2016-09-04 12:36:16

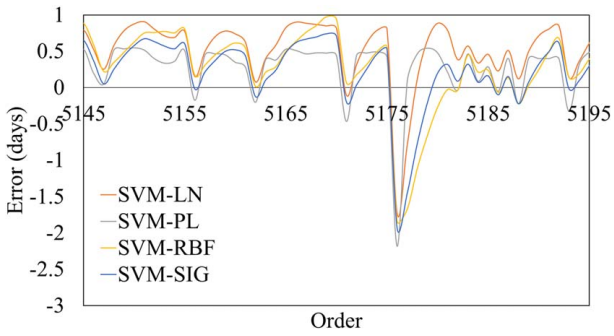

Fig. 12 Forecast error of $t+1$ in CA type 1

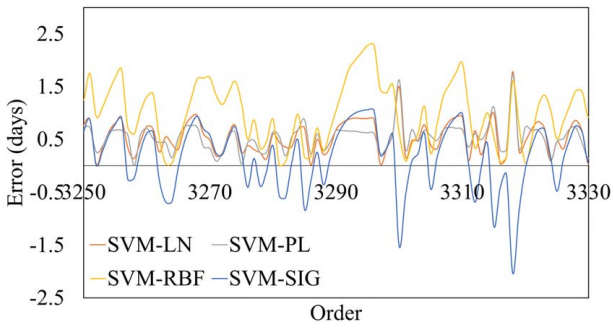

Fig. 13 Forecast error of $t+1$ in CA type 2

CC, the test results have a good forecasting performance, as shown in each Figure. Each SVM model based on different kernel functions catches the trend of observation. Also, when the time is increasing, the SVM-PL will give overestimated values for both products. Although the SVM-PL will overestimate values as time increases, the model does not lose its forecasting performance with higher failure time. In Fig. 9 on orders 5184 to 5189 and Fig. 11 on orders 3277 to 3,283, the SVM-PL with time $t+3$ provides a forecasting value near to the observation. The actual failure time and the forecasted failure time for these orders are shown in Table 9.

Since the observed trend is close to linear or polynomial function, SVM-LN and SVM-PL have a better performance than the other two models. SVM-PL is more suitable than SVM-LN since the trend of observation is like a polynomial function.

All models have a value of 1.0 for CC. They perform with similar trends, as shown in Figs. 8–11. Although all models have a similar trend, they do not guarantee small residual errors based on RMSE and MAE listed in Tables 7 and 8.

Figures 12 and 13 show the error between forecasting $t+1$ and observation for CA type 1 and CA type 2. SVM-PL has a better performance than others. In addition, the trend of error has a cycle period in both Figures. Figure 12 shows the models overestimate the actual day, but sometimes the models can catch the actual failure time. Figure 13 also shows a similar trend, such as error with the cycle period. Based on the current observation, future work suggests training an error model that can forecast the next error between forecasting and actual failure time to reduce the error between forecasting and observation.

The outcomes provide helpful insights into enhancing the sustainability of medical devices. For example, the forecasting results provide information on product maintenance needs and the degree of repairability. Also, predicting time between failures gives repair service providers and technicians sufficient advance notice for predicting the resources needed for repair and proper resource management for repair services. Moreover, the prediction outcomes can be used for forecasting the amount of waste generated if the malfunctioning medical devices would not be repaired. Forecasting waste provides further information on how to define strategies for the reduction of greenhouse gas (GHG) emissions.

5 Conclusion

This study aims to forecast the arrival time of the next repair order or the failure time by applying the SVM model into a medical device data set with over 530,000 records of repair and maintenance activities. Four SVM kernel functions, including SVM-LN, SVM-PL, SVM-RBF, and SVM-SIG, have been compared for forecasting the next failure time of two categories of products labeled as CA type 1 and CA type 2. The results reveal that the SVM-LN and SVM-PL perform well in forecasting the time of the next repair request or failure time. Among all functions, SVM-PL has the best forecasting performance based on the RMSE and MAE values for testing.

In addition, frequency analysis has been run to analyze the data further and identifies the best-fitted distributions to the failure count, the time between failure, and the time to repair. Four probability distributions, including Gumbel, Gamma, Normal, and Weibull distribution, have been analyzed. Analyzing the failure

count reveals that PA type 1 is more reliable among products with the same function. CA type 1 and PA type 1 have higher $P(X \geq 1)$ of TBF among all products in terms of random failure. M8 type 2 has a higher $P(X \geq 1)$ of TBF in terms of PD among other products with the same function. Finally, analyzing TTR reveals that CA type 1 and M8 type 2 are not easy to repair among all products.

The study shows the importance of machine learning tools such as SVM models in predicting the time of repair orders. Forecasting the time to failure and time to repair provides guidelines to designers for improving product repairability. The SVM model can further be used in forecasting the waste generation rate.

The study can be extended in several ways. First, other categories of products and types of failures can be compared together to identify the most vulnerable products and the type of repairs needed in each category. Second, the study outcome, which includes aftermarket repair and maintenance requests, can be linked to the product design features to identify design improvement directions. Third, the data analytics results can be fed to cost modeling techniques to quantify the business outcomes of repair services and identify the best repair strategies companies need to adopt. Decisions such as whether to handle repair services by in-house teams or outsource them to original equipment manufacturers or third-party repair service providers, depending on the demand and repair cost, can be informed by the current data analyses. Fourth, the study outcomes can be fed to resource allocation and scheduling models to help enterprises manage workforce requirements for repair services. Fifth, other machine learning tools can be employed to facilitate data analytics efforts. Finally, training an error model that can forecast the following error between forecasting and actual failure time will be further analyzed.

Acknowledgment

This material is based upon work supported by the National Science Foundation–USA under Grant Nos. CMMI-2017968 and CBET-2017971. Any opinions, findings, and conclusions, or recommendations expressed in this material are those of the authors and do not necessarily reflect the views of the National Science Foundation.

Conflict of Interest

There are no conflicts of interest.

Data Availability Statement

The data sets generated and supporting the findings of this article are obtainable from the corresponding author upon reasonable request.

Nomenclature

b = bias
d = degree term
n = number of the probability distribution parameters
r = scaling factor
s = the number of samples
x = input vector
v = number of support vector
$\boldsymbol{w}$ = weight of support vector machine
R = structural risk function
c^* = penalty parameter
$\hat{h}$ = the maximum value of the likelihood function
$\hat{y}$ = target data
x_k = support vector
a, a^* = Lagrange multipliers
$K(x, x_k)$ = Kernel function
$L_\varepsilon(\hat{y})$ = Vapnik's ε-insensitive loss function
ε = error tolerance
ξ, ξ^* = slack variables
$\Phi(x)$ = nonlinear function

References

[1] Kang, S., Kim, E., Shim, J., Chang, W., and Cho, S., 2018, "Product Failure Prediction With Missing Data," Int. J. Prod. Res., **56**(14), pp. 4849–4859.
[2] Song, S., Sheinin, D. A., and Yoon, S., 2016, "Effects of Product Failure Severity and Locus of Causality on Consumers' Brand Evaluation," Soc. Behav. Pers., **44**(7), pp. 1209–1221.
[3] Shaharudin, M. R., Tan, K. C., Kannan, V., and Zailani, S., 2019, "The Mediating Effects of Product Returns on the Relationship Between Green Capabilities and Closed-Loop Supply Chain Adoption," J. Cleaner Prod., **211**, pp. 233–246.
[4] Mastrucci, A., Marvuglia, A., Popovici, E., Leopold, U., and Benetto, E., 2017, "Geospatial Characterization of Building Material Stocks for the Life Cycle Assessment of End-of-Life Scenarios at the Urban Scale," Resour. Conserv. Recycl., **123**, pp. 54–66.
[5] Li, W., Bai, H., Yin, J., and Xu, H., 2016, "Life Cycle Assessment of End-of-Life Vehicle Recycling Processes in China—Take Corolla Taxis for Example," J. Cleaner Prod., **117**, pp. 176–187.
[6] Bovea, M. D., Ibáñez-Forés, V., and Pérez-Belis, V., 2020, "Repair vs. Replacement: Selection of the Best End-of-Life Scenario for Small Household Electric and Electronic Equipment Based on Life Cycle Assessment," J. Environ. Manage., **254**, p. 109679.
[7] Pandey, V., Thurston, D., and Jolly, M., 2006, "Remanufacture Dependency Matrix and Market Diffusion of Multi-Level Products," Proceedings of ASME 2006 International Design Engineering Technical Conferences and Computers and Information in Engineering Conference, Philadelphia, PA, Sept. 10–13, pp. 801–809.
[8] Behdad, S., Williams, A. S., and Thurston, D., 2012, "End-of-Life Decision Making With Uncertain Product Return Quantity," ASME J. Mech. Des., **134**(10), p. 100902.
[9] Yoon, K. B., and Sohn, S. Y., 2007, "Forecasting Both Time Varying MTBF of Fighter Aircraft Module and Expected Demand of Minor Parts," J. Oper. Res. Soc., **58**(6), pp. 714–719.
[10] Al-Garni, A. Z., Tozan, M., Al-Garni, A. M., and Jamal, A., 2007, "Failure Forecasting of Aircraft Air-Conditioning/Cooling Pack With Field Data," J. Aircr., **44**(3), pp. 996–1002.
[11] Wang, Q., and Yuan, H., 2017, "Failure Rate Prediction Based on AR Model and Residual Correction," 2017 Second International Conference on Reliability Systems Engineering (ICRSE), Beijing, China, July 10–12, pp. 1–5.
[12] Wang, J., and Yin, H., 2019, "Failure Rate Prediction Model of Substation Equipment Based on Weibull Distribution and Time Series Analysis," IEEE Access, **7**, pp. 85298–85309.
[13] Sexton, T., Hodkiewicz, M., Brundage, M. P., and Smoker, T., 2018, "Benchmarking for Keyword Extraction Methodologies in Maintenance Work Orders," PHM Society Conference, Philadelphia, PA, Sept. 24–27, Vol. 10, pp. 543–551.
[14] Brundage, M. P., Sexton, T., Hodkiewicz, M., Dima, A., and Lukens, S., 2021, "Technical Language Processing: Unlocking Maintenance Knowledge," Manuf. Lett., **27**, pp. 42–46.
[15] Muhammad, R., Yuan, X., Kisi, O., and Yuan, Y., 2017, "Streamflow Forecasting Using Artificial Neural Network and Support Vector Machine Models," Am. Sci. Res. J. Eng. Technol. Sci., **29**(1), pp. 286–294.
[16] Chang, M. J., Chang, H. K., Chen, Y. C., Lin, G. F., Chen, P. A., Lai, J. S., and Tan, Y. C., 2018, "A Support Vector Machine Forecasting Model for Typhoon Flood Inundation Mapping and Early Flood Warning Systems," Water, **10**(12), p. 1734.
[17] Zendehboudi, A., Baseer, M. A., and Saidur, R., 2018, "Application of Support Vector Machine Models for Forecasting Solar and Wind Energy Resources: A Review," J. Cleaner Prod., **199**, pp. 272–285.
[18] Gentile, M., and Summers, A. E., 2006, "Random, Systematic, and Common Cause Failure : How Do You Manage Them ?," Process Saf. Prog., **25**(4), pp. 331–338.
[19] Ic, N., Cc, N., Ad, O., and Luntsi, G., 2017, "Failure Mode Analysis of Radiologic Equipment in a Tertiary Institution in South-Eastern Nigeria," J. Dent. Med. Sci., **16**(10), pp. 82–90.
[20] Patil, R. B., 2019, "Integrated Reliability and Maintainability Analysis of Computerized Numerical Control Turning Center Considering the Effects of Human and Organizational Factors," J. Qual. Maint. Eng., **26**(1), pp. 87–103.
[21] Lampreia, S., Vairinhos, V., Lobo, V., and Requeijo, J., 2019, "A Statistical State Analysis of a Marine Gas Turbine," Actuators, **8**(3), p. 54.
[22] Sukhwani, H., Alonso, J., Trivedi, K. S., and McGinnis, I., 2016, "Software Reliability Analysis of NASA Space Flight Software: A Practical Experience," 2016 IEEE International Conference on Software Quality, Reliability and Security (QRS), Vienna, Austria, Aug. 1–3, pp. 386–397.
[23] Tronskar, J. P., Li, Z., and Edwards, J. D., 2005, "Probabilistic Integrity Assessment of Pipelines and Pressure Vessels With Localized Corrosion," International Conference on Offshore Mechanics and Arctic Engineering, Halkidiki, Greece, June 12–17, vol. 3, pp. 275–287.
[24] Akaike, H., 1998, "Information Theory and an Extension of the Maximum Likelihood Principle," *Selected Papers of Hirotugu Akaike*, E. Parzen, K.

Tanabe, and G. Kitagawa, eds., Springer New York, New York, NY, pp. 199–213.
[25] Schwarz, G., 1978, "Estimating the Dimension of a Model," Ann. Stat., **6**(2), pp. 461–464.
[26] Mutua, F. M., 1994, "The Use of the Akaike Information Criterion in the Identification of an Optimum Flood Frequency Model," Hydrol. Sci. J., **39**(3), pp. 235–244.
[27] Haddad, K., and Rahman, A., 2011, "Selection of the Best fit Flood Frequency Distribution and Parameter Estimation Procedure: A Case Study for Tasmania in Australia," Stoch. Environ. Res. Risk Assess., **25**(3), pp. 415–428.
[28] Rahman, A. S., Rahman, A., Zaman, M. A., Haddad, K., Ahsan, A., and Imteaz, M., 2013, "A Study on Selection of Probability Distributions for at-Site Flood Frequency Analysis in Australia," Nat. Hazards, **69**(3), pp. 1803–1813.
[29] Alam, M. A., Farnham, C., and Emura, K., 2018, "Best-Fit Probability Models for Maximum Monthly Rainfall in Bangladesh Using Gaussian Mixture Distributions," Geosciences, **8**(4), pp. 1–15.
[30] Vapnik, V. N., 1995, *The Nature of Statistical Learning Theory*, Springer-Verlag New York, Inc., New York.
[31] Al-Shammari, E. T., Mohammadi, K., Keivani, A., Hafizah, Ab Hamid, S., Akib, S., Shahaboddin, S., and Petković, D., 2016, "Prediction of Daily Dewpoint Temperature Using a Model Combining the Support Vector Machine With Firefly Algorithm," J. Irrig. Drain. Eng., **142**(5), pp. 1–9.
[32] Xiao, J., Zhu, X., Huang, C., Yang, X., Wen, F., and Zhong, M., 2019, "A New Approach for Stock Price Analysis and Prediction Based on SSA and SVM," Int. J. Inf. Technol. Decis. Mak., **18**(1), pp. 35–63.
[33] Wang, J. H., Lin, G. F., Chang, M. J., Huang, I. H., and Chen, Y. R., 2019, "Real-Time Water-Level Forecasting Using Dilated Causal Convolutional Neural Networks," Water Resour. Manag., **33**(11), pp. 3759–3780.
[34] Cristianini, N., and Shawe-Taylor, J., 2000, *An Introduction to Support Vector Machines and Other Kernel-Based Learning Methods*, Cambridge University Press, Cambridge, MA.
[35] Bard, J. F., 1983, "An Efficient Point Algorithm for a Linear Two-Stage Optimization Problem," Oper. Res., **31**(4), pp. 670–684.